Predicting Tumor Mutational Burden from Liver Cancer Pathological Images Using Convolutional Neural Network

Hong Zhang[1,2], Fei Ren[2], Zhonglie Wang[2,7], Xiaosong Rao[4], Li Li[5], Junbo Hao[6], Rui Yan[2,7], Jiancheng Luo[3*], Ming Du[1*], Fa Zhang[2*]
[1]College of Computer Science and Technology, Donghua University, Shanghai, China
[2]High Performance Computer Research Center, Institute of Computing Technology, Chinese Academy of Sciences, Beijing, China
[3]Aiyi Technology Co.,Ltd, Beijing, China
[4]Department of Pathology, Peking University International Hospital, Peking University, Beijing, China
[5]Department of Oncology, Peking University International Hospital, Peking University, Beijing, China
[6]School of Electronic Engineering, Xidian University, Xi'an, China
[7]College of Computer Science and Technology, Anhui University, Hefei, China
luojc@aiyi.link, duming@dhu.edu.cn, zhangfa@ict.ac.cn

***Abstract*—Tumor mutational burden (TMB) is the most important and most promising biomarker in the era of tumor immunotherapy, and it can predict the immunotherapy efficiency of patients in various cancers including liver cancer. TMB is mainly obtained by next generation sequencing technology such as whole exome sequencing (WES). However, conditions such as excessive testing costs, lengthy detection cycles, and tissue sample dependence severely limit the clinical application of TMB. Inspired by the inner link between the intrinsic characteristics of the tumor cell genome and the pathological features of tumor cells and their microenvironment-related cells, we propose a deep learning method for predicting the level of TMB (high or low) directly from pathological images. This study found that the feature scale (receptive field) is the biggest factor affecting the classification effect of TMB prediction, and further determined the best receptive field through a series of experiments. Experimental results show that our method is far more out performance of the commonly used panel sequencing (99.7% VS 79.2%). To the best of our knowledge, this is the first research to predict TMB and the highest level of accuracy of genomic characteristic predicted by pathological images. The proposed method has the potential to provide immunotherapy to a much broader subset of patients with liver cancer.**

Keywords—tumor mutational burden, liver cancer, receptive field, pathological image, convolutional neural network

I. INTRODUCTION

With the immune-checkpoint antibodies such as PD-1, PD-L1, and CTLA-4 monoclonal antibodies approved by the FDA for various tumors such as lung cancer, melanoma, and liver cancer based on survival benefit, the clinical practice of cancer treatment has entered a new era of "immunotherapy" [1][2][3]. Unfortunately, only a small percentage of patients benefit from immunotherapy, and the development, optimization, and application of predictive biomarkers has become a top priority. Tumor mutational burden (TMB) is an important biomarker in the era of tumor immunotherapy. Based on the validation of the predictive power of TMB immunotherapy in clinical trials CheckMate-227 and CheckMate-026, TMB officially entered the 2019 version of the NSCLC "NCCN" guidelines, becoming part of the clinical practice. It is worth noting that the predictive power of TMB in immunotherapy is not limited to "hot tumors" such as NSCLC and melanoma, but is a biomarker for pan-cancer, and has predictions ability in various tumors including liver cancer. [4][5]. A meta-study of 45 studies with over 100,000 patients found that TMB not only predicts OS, PFS, and ORR in immunotherapy patients, but also finds high levels TMB of non-immunotherapy liver cancer, NSCLC, and melanoma is associated with poor survival [6].

TMB is mainly obtained by next generation sequencing methods such as whole exome sequencing. However, conditions such as excessive testing costs, lengthy turnaround time, and tissue sample dependence severely limit the clinical application of TMB. Usually, the cost of obtaining a TMB score is several to ten thousand dollars, tens to hundreds of times the cost of pathological diagnosis, which poses a major obstacle to the selection of TMB testing in many patients. In addition, the mean turnaround time for TMB scoring is 2 to 3 weeks, especially for WES testing, it may take up to one months, which falls outside the window for treatment decisions recommended by the College of American Pathologists. Moreover, obtaining a TMB score requires a sufficient number and quality of tissue samples, which further limits the patient to achieve it. During the actual operation of the clinical trial, the failure rate for obtaining a TMB score was 42% in CheckMate-227 and 34% in CheckMate-568[7]. Therefore, the development of low-cost, fast, and independent sample-free TMB score acquisition means has great clinical application value. TMB prediction based on pathological image using deep learning is one of the potential means.

Deep learning is end-to-end learning that automatically extracts features. The most widely used convolutional neural network (CNN) was used to process natural images, and later applied to remote sensing, medicine and other fields. CNN is also often used to histology images for pathological diagnosis classification. With the rapid development of precision medicine, the genomic information of tumors plays an increasingly important role in the clinical diagnosis and treatment of tumors. Whether the genome-related feature information of tumors can be directly extracted from pathological images has become a problem worth exploring. The latest research found that deep learning can not only predict the information of EGFR and other driving gene mutations from pathological images with high accuracy, but also can predict the MSI status related to tumor immunity [8][9]. From the perspective of tumor evolutiology and tumor

*Corresponding author.

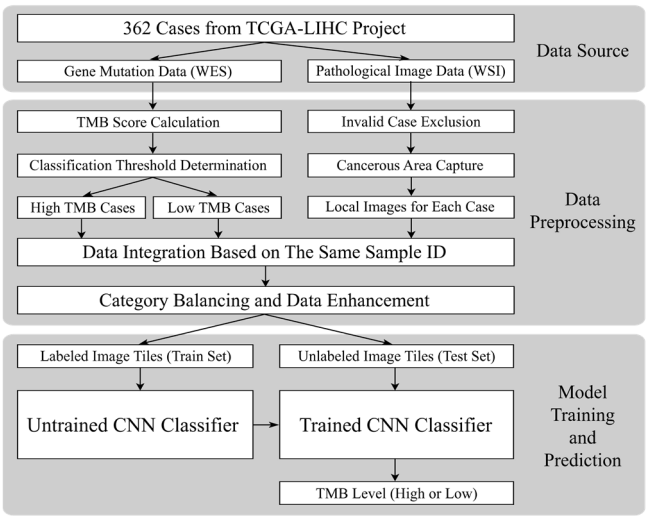

Fig. 1. Flowchart illustrating the method overview.

ecology, the spatial structure of tumor cells and immune cells, the pathological features of tumor cells and their microenvironment-related cells, and the intrinsic characteristics of tumor cells must have the universal internal connection and the classification framework of tumor evolution and features proposed by experts in related fields have laid a theoretical foundation [10]. TMB, as a surrogate marker of the most critical "grasping" neoantigen in the interaction between tumor cells and immune cells, is an important evaluation index of the immunogenicity of tumor cells, that is, the "harm degree" of the immune system faced by tumor cells, and should also be presented in its pathological images.

This study designed a CNN-based classifier to predict the level of TMB (high or low) by classifying liver cancer pathological images, thus establishing a mapping from pathological image data to TMB. This study not only explored the gene mutation information hidden in the HE pathological images, but also found the best CNN receptive field, which can infer the best feature scale for mining TMB information in liver cancer pathological images. Experiments show that the accuracy of the model on the test set is 0.9486, and the AUC value is 0.9488, and the patient survival prediction by this model is obviously better than the method for estimating TMB based on panels. To the best of our knowledge, this is the first research to predict TMB by the pathological images and the highest level of accuracy of genomic characteristic predicted by pathological images.

II. Materials and Methods

The accumulation of gene mutations in somatic cells leads to the production of tumor cells. TMB is an indicator of the degree of gene mutation in tumor cells, which can reflect the pathogenesis of tumors at the molecular level. The pathomorphological features of tumor cells and their microenvironment-related cells are generally intrinsically linked to the intrinsic characteristics of tumor cells genomes, which led us to elucidate the idea of predicting TMB values through pathological image features.

In order to achieve this goal, we designed the overall method flow as shown in Fig. 1. We first preprocessed gene mutation data and pathological image data of 362 cases separately, and then integrated the obtained TMB data and image data into the training of CNN classifier. The methods are described in detail below.

A. TMB Level Annotation for 362 Cases

We conducted research using data from the TCGA-LIHC project of The Cancer Genome Atlas (TCGA) program. Somatic mutation (SNPs and small INDELs) were retrieved from GDC TCGA Liver Cancer (LIHC) hub using UCSC Xena browser. The MuSE Variant Aggregation and Masking results of 362 samples were used in this study. Only variants labeled with a PASS filter tag, located in exon region and not the synonymous effect variant, or located in the splice region, were utilized to calculate TMB.

Before classifying TMB, we need to choose a threshold to distinguish between TMB high or low, while liver cancer does not currently have a TMB threshold that is clinically significant. Reference[11] proposes the use of segmented regression or “broken-stick analysis” to find the threshold by finding an inflection point. This study used this threshold setting method.

Then we sorted the TMB scores of 362 cases in reverse order, drew them as a scatter plot, and applied segmented regression to fit the scatter with two straight lines, and finally find the inflection point of the curve (as shown in Fig. 2). According to this inflection point, we classified the TMB results of 362 cases into high and low levels. There are 32 cases in the high level of TMB and 330 cases in the low level of TMB.

B. Pathological Image Data Preprocessing

Pathological images of liver cancer are obtained from tissue samples of the liver of patients, which are processed by a series of techniques including dehydration, wax immersion, embedding, sectioning and staining. The accuracy of pathological images can reach the cellular level, which can help doctors make judgments about liver cancer from a more essential perspective. We used the GDC tool to download 380 whole slide images (WSI) of 362 patients with liver cancer from the TCGA-LIHC project. The pathological images are RGB three-channel bitmap images based on mature HE staining technique, which corresponded to the samples of somatic mutation data mentioned above. We excluded 12 images of 12 cases due to image quality reasons at the pathologist's suggestion.

In the dataset, the whole slides were imaged using a digital slide scanner at 200× or 400× magnification. Comparing different magnifications, 200× is the best practice for doctors to distinguish between benign and malignant

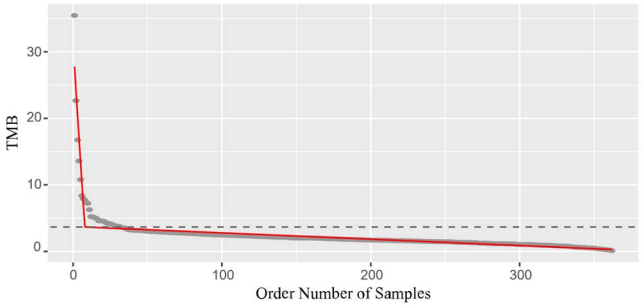

Fig. 2. The TMB scatter plot of 362 cases. The red lines are the result of segmented regression. The inflection point corresponds to a TMB value of approximately 3.66. The gray horizontal dashed line passes the inflection point, and there are 32 points above this line, indicating that the TMB scores of the corresponding cases are at a high level.

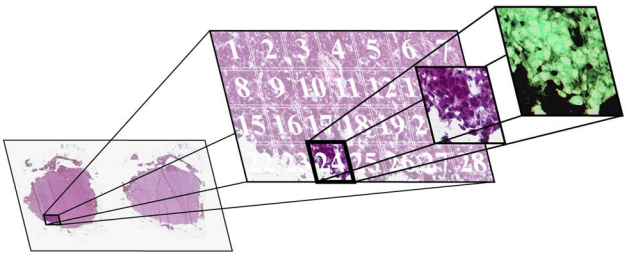

Fig. 3. The preparation process of the pathological image dataset, taking an image in negative category as an example.

tumors under the microscope. A team of pathologists cut out several local images in each slide at 200× magnification using Aperio ImageScope. The size of each local image is 1712×961 pixels, and only a cancer tissue region is included in each local image. As a result, we obtained 470 local images with the high TMB label, and 5162 local images with the low TMB label.

If the local images are directly used for the training of the deep learning model, we will face the problem of excessive resolution and unbalanced categories. Therefore, we use the sliding window method to perform tile segmentation, and achieve data enhancement by flexibly adjusting the step size. The size of the window we used is 256×256 pixels. For the local images of low TMB cases, 28 tiles (4 rows and 7 columns) were cut out from each local image. Although there are small overlaps between each tiles, they are already the smallest overlapping areas, without missing any pixel. For the local images of high TMB cases, 300 small tiles (12 rows and 25 columns) which retained a larger proportion of overlapping areas were cut out from each local image. Thus, the positive (high TMB) category has 141,000 tiles, and the negative (low TMB) category has 144,536 tiles. The number of tiles in the two categories is approximately the same, so the problem of category imbalance is solved while the data is enhanced. Then we inverted the color of all the tiles. The entire process is shown in Fig. 3.

Finally, the training set and test set are randomly divided by a ratio of 4:1 at the tiles level.

C. CNN-based Image Classifier

In the field of image classification, convolutional neural networks (CNN) and its derived models are widely used. CNN is a feedforward neural network whose history dates back to 1962. Biologists Hubel and Wiesel discovered that the cells in the cat's visual cortex are sensitive to parts of the visual input, and accordingly the concept of receptive field was proposed [12]. In 1980, Kunihiko Fukushima proposed the neocognitron based on Hubel and Wiesel's local receptive field theory. This is the earliest implementation of the CNN network model [13].

Receptive field is a basic concept of convolutional neural networks. Unlike a fully connected network whose features all depend on the overall input, each neuron in the convolutional layer only establishes a connection with the neurons in the upper receptive field through the convolution kernel [14]. This area is the receptive field of the neuron. The advantage of convolutional neural networks is the weight sharing and local connection which absorbs the idea of local receptive field. CNN can effectively control the parameter size and the amount of calculation while ensuring the training effect.

After trying out several popular CNN-based models such as AlexNet, VGG, and ResNet, we found that the phenomenon of over-fitting was very serious which was embodied in the gradual convergence of accuracy and loss values in the training set, but not the test set. After analysis, these models were proposed to extract features of natural images rather than pathological images. Relatively speaking, they pay more attention to the connection between the subject and the environment in the image. Therefore, the receptive fields of these models are very large, and each feature in the resulting feature map contains a wide range of information, even global features. For example, the pixel on the feature map of AlexNet's $pool_5$ output is 195×195 pixels on the input image[15], the maximum receptive field of VGG16 is 212×212 pixels, and the maximum receptive field of ResNet50 can reach 483×483 pixels.

However, the problem of predicting TMB high or low from pathological images is quite different from the natural image classification problem, because pathological image classification (such as cancer grading) pays more attention to minute details than natural image classification (such as cat and dog classification). We decided to narrow the scope of the receptive field and simplify the model, using the collection of local features as the credentials of the classification to adapt to the classification problem of the pathological images, while alleviating the over-fitting problem.

After testing different hyperparameters, we finally chose 4 pairs of convolution layer and max pooling layer, and connected a fully connected layer with 256 neurons (the dropout fraction of the input is 0.5 to prevent over-fitting). ReLU is used as the activation function in both the convolution layers and the fully connected layer. The last layer contains only one neuron, and Sigmoid is used as the activation function, with the output of the last layer as the classification standard. The model structure diagram is shown in Fig. 4. We used the cross-entropy loss function and the Adam optimization algorithm for model training.

III. Results

A. Receptive Field Determination

In this study, the choice of receptive field size is an important issue, which is related to the exploration of the feature scale in the liver cancer pathological images which are used to predict TMB levels. In the experiment, we can adjust the size of the receptive field by adjusting the depth of the CNN model and the size of the convolution kernel. However, as the depth of the model changes, the number of model

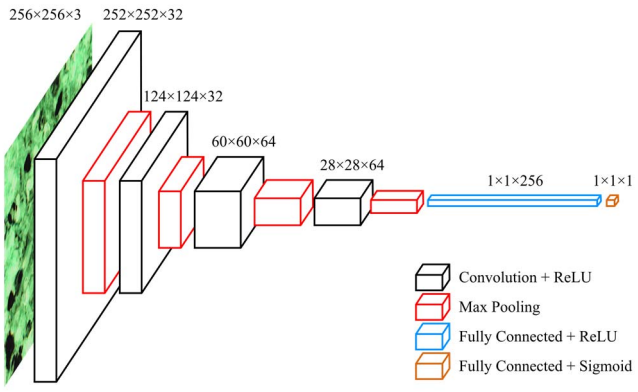

Fig. 4. Structure diagram of our classification model.

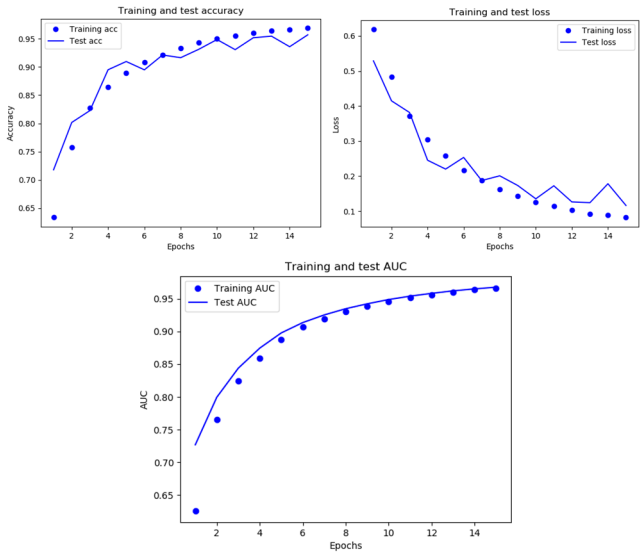

Fig. 5. Accuracy curve, loss curve and AUC curve.

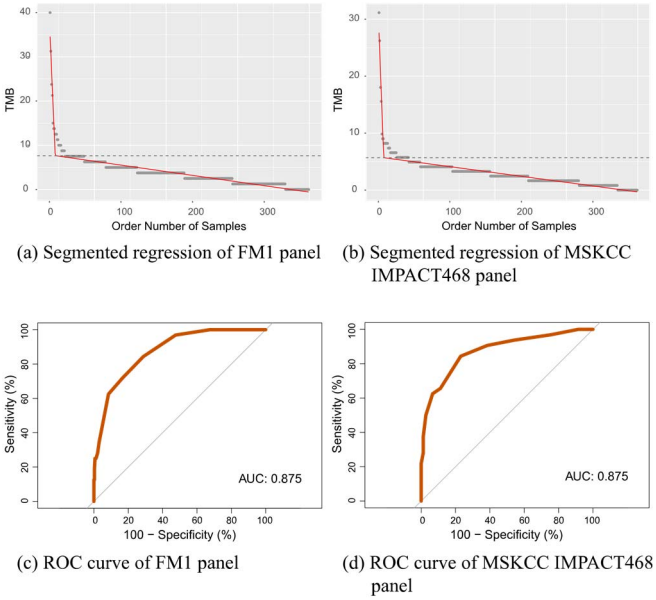

(a) Segmented regression of FM1 panel (b) Segmented regression of MSKCC IMPACT468 panel

(c) ROC curve of FM1 panel (d) ROC curve of MSKCC IMPACT468 panel

Fig. 6. Related diagrams of TMB classification by two panels. The segmentation thresholds were found by segmented regression using two panels to find the inflection points and the results are shown in (a) and (b), where the TMB score of the inflection point calculated by FM1 panel is 7.65, and the TMB score of the inflection point calculated by MSKCC IMPACT468 panel is 5.64. (c) and (d) are ROC curve plots of TMB classification using two panels.

parameters changes significantly, which greatly affects the training effect (it may lead to over-fitting or under-fitting problem). Therefore, we mainly used the method of changing the size of the convolution kernel to control the receptive field.

We ran a series of experiments to evaluate our method. First, by substantially changing the receptive field (from 10×10 pixels to 212×212 pixels), the appropriate range of receptive field is locked between 46×46 pixels and 60×60 pixels according to the generalization effect of each model. Through comparative experiments, we found that if the model's receptive field is outside this range, serious over-fitting or under-fitting problems will occur. Then, on the premise that the number of convolutional layers and receptive field range are fixed, we use different convolution kernel sizes to control the receptive field in a more fine-grained way. We designed 8 models by extracting several of the 3 convolution kernels which belongs to the first 3 convolution layers and changed their size from 3×3 to 5×5. These models are shown in Table I.

After the 8 models were trained with the same dataset, the accuracy and AUC of each model are shown in Table II. According to the experimental results, the best model is RF48, and the best receptive field is 48×48 pixels.

B. *Prediction of Individual Tiles and Cases*

After determining the receptive field and training the model using the dataset mentioned in Chapter II, we plot the accuracy, loss and AUC curves as shown in Fig. 5. We used the results of the 10th epoch of training, the accuracy on the test set is 0.9486, and the AUC value is 0.9488.

Based on the trained model, we made a prediction for all 350 cases. An average of 816 tiles were cut out for each case. After predicting the TMB level for each tile of a case, we used the majority voting method to calculate the overall TMB level of the current case. After the experiment, only one of the 350 cases predicted errors and belonged to the false negative category, The classification accuracy of TMB prediction at patient level is 0.9971, achieving an amazing high level.

C. *Prediction of Normal Tissue Tiles*

To further test the validity of this model, we also used normal tissue local images for prediction. Since the normal tissue regions of the pathological images had been excluded during the data pre-processing, they had not participated in the training. We cut the normal tissue local images collected into 768 tiles for prediction (the label is unified to low TMB). As a result, 3 tiles were mispredicted as high TMB with an accuracy of 0.9961.

TABLE I. 8 MODELS WITH DIFFERENT RECEPTIVE FIELDS

Model ID	Kernel Sizes of 4 Convolution Layers				RF (pixel)
	Kernel 1	*Kernel 2*	*Kernel 3*	*Kernel 4*	
RF46	3×3	3×3	3×3	3×3	46×46
RF48	5×5	3×3	3×3	3×3	48×48
RF50	3×3	5×5	3×3	3×3	50×50
RF52	5×5	5×5	3×3	3×3	52×52
RF54	3×3	3×3	5×5	3×3	54×54
RF56	5×5	3×3	5×5	3×3	56×56
RF58	3×3	5×5	5×5	3×3	58×58
RF60	5×5	5×5	5×5	3×3	60×60

TABLE II. ACCURACY AND AUC VALUES FOR 8 MODELS

Model ID	RF (pixel)	Test Accuracy	Test AUC
RF46	46×46	0.9232	0.9215
RF48	48×48	0.9486	0.9488
RF50	50×50	0.9315	0.9175
RF52	52×52	0.8765	0.8846
RF54	54×54	0.8823	0.8804
RF56	56×56	0.8697	0.8783
RF58	58×58	0.8754	0.8729
RF60	60×60	0.9033	0.8700

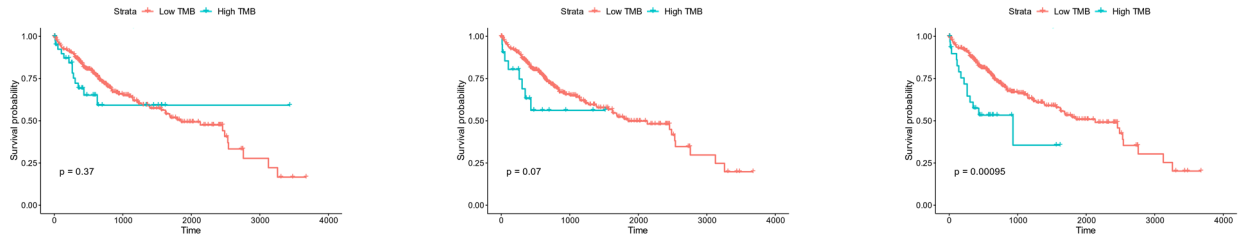

(a) Survival analysis based on MSKCC IMPACT468 panel

(b) Survival analysis based on FM1 panel

(c) Survival analysis based on the prediction of our CNN model

Fig. 7. Comparison of the methods of two panels and our model for survival analysis.

D. Comparison with the Panel Method

Since most of the clinically referenced TMB scores are now obtained by gene panels, the TMB obtained in this way (panel TMB) is an approximation of the TMB obtained by WES(WES TMB). At present, the FDA has approved the two panels of MSKCC IMPACT468 and FM1. We extracted the genes in these two panels from the TCGA-LIHC project and calculated the TMB scores of these panels.

Based on the classify status determine by WES TMB inflection point value mentioned in Chapter 2, we compared the TMB classification accuracy between predicted by the trained CNN model and predicted by the panel TMB. As shown in Fig. 6, the classification accuracy and AUC value of FM1 panel for TMB are 0.807 and 0.875. Similarly, the classification accuracy and AUC value of MSKCC IMPACT468 panel for TMB are 0.778 and 0.875, which is far lower than the corresponding score predicted by the trained CNN model.

Previous studies have found that high TMB in liver cancer is associated with poor prognosis, so we compared the survival predictive ability between panel TMB and TMB predictive classification based on CNN model. Firstly, we use segmented regression to find the inflection point of corresponding classification for panel TMB. It can be seen from the graph that TMB between adjacent patients is over-fitted to the same value due to the limitation of the testing area, especially in patients with lower TMB, which is a direct reflection of the lower accuracy of panel TMB. Survival curve analysis showed that there was significant difference in survival time between high TMB group and low TMB group (mOS=357d vs 624d, p=0.00095), but there was no difference between high TMB group and low TMB group, whatever use the FM1 panel or MSKCC IMPAT468 panel (as shown in Fig. 7). Obviously, our CNN model shows good performance and is more helpful for the prognosis of patients.

Experiments have shown that our classification model can extract the features of liver cancer pathological images well, and thus classify the TMB levels of cancer tissues in high or low. The patient survival prediction by this model is better than the method for estimating TMB based on panels.

E. Pathological Interpretation

Inspired by the inner link between the intrinsic characteristics of the tumor cell genome and the pathological features of tumor cells and their microenvironment-related cells, we propose a deep learning method for predicting the level of TMB (high or low) directly from the pathological images. For routine diagnosis, HE staining is the preferred way to observe cellular and tissue structure detail by pathologists, because it can demonstrate a broad range of cytoplasmic, nuclear, and extracellular matrix features under electron microscopy. At high magnification, the cells of liver cancer shows morphological changes, such as increased size, deeply stained nucleus and many mitoses. A detailed pathological features comparison table, as shown in Table III, is produced based on the clinical pathologists experience on distinguishing the normal cells and cancer cells in liver cancer.

Different receptive fields can obtain information on different scales, and small receptive fields will better obtain

TABLE III. PATHOLOGICAL FEATURES OF NORMAL CELLS AND LIVER CARCINOMA CELLS

Item	Normal Cells	Liver Carcinoma Cells
Cellular Size	Small	Big
Cellular Shape	Uniform Size	Uneven size, Pleomorphic, tumor giant cells may be present
Nuclear Size	Small	Enlarge
Nuclear Shape	Circular or Ovoid	Irregular
Cytoplasm	Scanty	Irregular distribution, granular
Hyperchromasia	Rare	Common
Nuclear/Cytoplasmic Ratio	Normal	Enlarge
Nucleolus	Small, regular shape, limited amount	Enlarge, irregular shape, increase in numbers
Mitoses	May be present	Common, pleomorphic

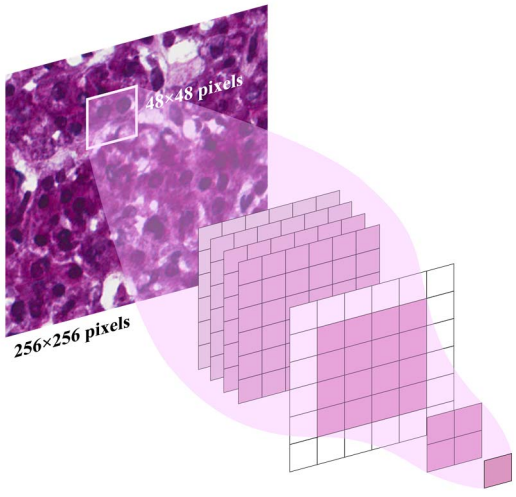

Fig. 8. The scale of the optimal receptive field on the input image.

local information. In HE slides under 20× field of view, the morphological characteristics of cancer cells belong to local information, so a smaller receptive field can be used to obtain better prediction results. Fig. 8 shows an example area where the 48*48 pixel receptive field is projected onto the input image. In a 20× pathological image, the receptive field of this size contains approximately 2 cells. this receptive field size can help the model to fully recognize the heterogeneity of liver cancer cells while avoiding the interference of interstitial tissues that may appear in the pathological images.

IV. Discussion

TMB is a biomarker that evolves quickly and compromises and balances according to the actual situation of clinical practice. The original definitions and findings of TMB are derived from the whole exome sequencing. Excessive cost and lengthy turnaround time limit the application of whole exome sequencing testing in clinical trials and clinical practice, while large panel tested hundreds of genes achieving some kind of balance between accuracy and clinical enforceability [16]. It is worth noting that hundreds of genes are tens of times different from the human body's own more than 20,000 genes. Panel TMB is equivalent to the results of the WES TMB sample survey, which introduces errors. Our experiments found that At present, there are only two FDA-approved panels: MSK IMPACT468 and FM1. In the threshold set by this study, the classification accuracy is only 80.7% and 77.8%, respectively, which is far lower than the classification accuracy of TMB predicted by pathological images. Compared with the higher accuracy of the panel TMB commonly used in clinical practice, the convenience and low cost of the deep learning algorithm itself are further accumulated. The use of deep learning to predict TMB through pathological images has a good clinical application prospect.

Although our method attained such high accuracy and exceeded the previously reported performance of predicting genomic features from histology[7][8], there are some limitations must to be pointed out. This method can only predict the classification of TMB, but cannot directly predict the TMB score. However, currently there is no threshold of clear clinical significance for liver cancer, which limits the clinical application value of this method at the present stage. The effect of deep learning is often directly affected by data. The method of our research is also required to be further verified in more independent data and more types of cancers. In order to avoid introducing too many errors in the data processing, pathologists were adopted to manually capture tumor area in this study, which reduced the convenience of this method to some extent. In the future, we will extend the study to other cancers to verify the effectiveness of the method, and TMB prediction algorithm based on automatic identification of tumor area needs to be further developed.

It is particularly noteworthy that this study found that the feature scale (receptive field) is the biggest factor affecting the classification effect of TMB prediction, and further explores the best receptive field through a series of experiments. With the gradual development of immunotherapy, especially the combination therapy has gradually become the mainstream, tumor immunotherapy requires the integration of multi-dimensional biomarkers to evaluate and predict gradually become the consensus of everyone [17]. The study of feature scales is likely to be an important research direction for the correlation prediction of genomic features and image data such as CT images and pathological images. This study lays an important foundation for further optimizing the predictive efficacy of pathological image TMB and constructing a clinical decision model for multimodal data integration such as tumor genomics and pathological imaging.

Acknowledgment

This research is supported by Peking University International Hospital Research Grant (No. YN2018ZD05), the National Key Research and Development Program of China (No. 2017YFE0103900 and 2017YFA0504702), the NSFC projects Grant (No. U1611263, U1611261, 61932018 and 61672493), and Beijing Municipal Natural Science Foundation Grant (No. L182053).

References

[1] N. Rizvi, L. Crinò, G. R. Blumenschein, S. J. Antonia, and C. Dorange, "Nivolumab versus Docetaxel in Advanced Nonsquamous Non–Small-Cell Lung Cancer," pp. 1–13, 2015.

[2] M. A. Postow et al., "Nivolumab plus Ipilimumab in Advanced Melanoma," 2013.

[3] A. B. El-khoueiry et al., "Nivolumab in patients with advanced hepatocellular carcinoma *(CheckMate 040)*: an open-label, non-comparative, phase 1/2 dose escalation and expansion trial," Lancet, vol. 389, no. 10088, pp. 2492–2502, 2017.

[4] R. Cristescu et al., "Pan-tumor genomic biomarkers for PD-1 checkpoint blockade-based immunotherapy," Science *(80-.).*, vol. 362, no. 6411, 2018.

[5] R. M. Samstein et al., "Tumor mutational load predicts survival after immunotherapy across multiple cancer types," Nat. Genet., 2019.

[6] D. Cao, H. Xu, X. Xu, T. Guo, and W. Ge, "High tumor mutation burden predicts better efficacy of immunotherapy : a pooled analysis of 103078 cancer patients," Oncoimmunology, vol. 0, no. 0, pp. 1–12, 2019.

[7] W. G. J. Addeo A, Banna G L, "Tumor Mutation Burden — From Hopes to Doubts," JAMA Oncol., vol. 5, no. 7, pp. 934–935, 2019.

[8] N. Coudray et al., "Classification and mutation prediction from non–small cell lung cancer histopathology images using deep learning," Nat. Med., vol. 24, no. October, 2018.

[9] J. N. Kather et al., "Deep learning can predict microsatellite instability directly from histology in gastrointestinal cancer."

[10] C. C. Maley et al., "Classifying the evolutionary and ecological features of neoplasms," Nat. Rev. Cancer, vol. 17, no. 10, pp. 605–619, 2017.

[11] B. B. Campbell et al., "Comprehensive Analysis of Hypermutation in Human Cancer," Cell, vol. 171, no. 5, pp. 1042–1056, 2017.

[12] E. R. Kandel, "An introduction to the work of David Hubel and Torsten Wiesel," J. Physiol., vol. 587, no. 12, pp. 2733–2741, 2009.

[13] K. Fukushima and S. Miyake, "Neocognitron: A Self-Organizing Neural Network Model for a Mechanism of Visual Pattern Recognition," [M]//Competition Coop. neural nets. Springer, Berlin, Heidelberg, pp. 267–285, 1982.

[14] H. G. E. Krizhevsky A, Sutskever I, "ImageNet Classification with Deep Convolutional Neural Networks," [C]//Advances neural Inf. Process. Syst., pp. 1097-1105., 2012.

[15] R. Girshick, J. Donahue, T. Darrell, J. Malik, and U. C. Berkeley, "Rich feature hierarchies for accurate object detection and semantic segmentation," 2012.

[16] M. Landscape, M. C. Revealed, and P. C. Sequencing, "Mutational Landscape of Metastatic Cancer Revealed from Prospective Clinical Sequencing of 10,000 Patients," Nat Med., vol. 23, no. 6, pp. 703–713, 2017.

[17] J. Galon and D. Bruni, "Approaches to treat immune hot, altered and cold tumours with combination immunotherapies," Nat. Rev. Drug Discov., p. 1, 2019.